Hindawi
Advances in Polymer Technology
Volume 2019, Article ID 8720678, 8 pages
https://doi.org/10.1155/2019/8720678

Research Article

Dielectric Properties of Two-Dimensional Bi_2Se_3 Hexagonal Nanoplates Modified PVDF Nanocomposites

Zunpeng Feng, Yanan Hao, Jiameng Zhang, Jing Qin, Limin Guo, and Ke Bi

State Key Laboratory of Information Photonics and Optical Communications, School of Science, Beijing University of Posts and Telecommunications, Beijing 100876, China

Correspondence should be addressed to Yanan Hao; hyn@bupt.edu.cn

Received 5 April 2019; Revised 21 May 2019; Accepted 13 June 2019; Published 3 July 2019

Academic Editor: Kinga Pielichowska

Topological insulator two-dimensional (2D) Bi_2Se_3 hexagonal nanoplates, which are highly insulating in the bulk and have a conductive topological surface state, have been prepared via an "EG- (ethylene glycol-) sol" method and characterized by transmission electron microscopy (TEM), X-ray diffraction (XRD), and scanning electron microscopy (SEM). Bi_2Se_3/PVDF (polyvinylidene fluoride) nanocomposites with various Bi_2Se_3 contents have been fabricated by a tape-casting method. The microstructure and dielectric performance of the Bi_2Se_3/PVDF nanocomposites are studied. The dielectric constant of the dense nanocomposite films keeps a relatively low value of about 16 when the Bi_2Se_3 content is lower than 12 vol.% then suddenly increases to 36 with a critical Bi_2Se_3 content of 13 vol.% due to the percolation effect of the large aspect ratio of the 2D Bi_2Se_3 nanoplates. The study of the Bi_2Se_3/PVDF nanocomposite system is conducive to the exploration of high-performance dielectrics.

1. Introduction

Materials with high permittivity and excellent dielectric properties have drawn extensive attention because of their growing demand in the applications of embedded capacitors, printed circuit boards (PCB) [1], microelectromechanical systems (MEMS) [2], field-effect transistors (FETs) and actuators, etc. [3]. As one of the most representative and widely used dielectric materials, ceramic-based dielectric materials have defects such as high brittleness and poor organic compatibility. Polymer-based dielectric materials have good flexibility, light weight, and good compatibility but a quite low dielectric constant (approximately 2 to 10). Therefore, a variety of high dielectric constant or conductive fillers are used to improve the dielectric properties of the polymers, such as high-k ceramic nanoparticles [4], metal nanoparticles, carbon nanotubes (CNTs) [1], and graphene nanosheets (GNs) [5].

In ceramic/polymer composites, it is necessary to use a high loading of ceramic nanoparticles (over 40 vol.%) as fillers to achieve a permittivity higher than 50, while the high loading of ceramic fillers usually results in poor processability and mechanical flexibility [6]. In order to solve these problems, a feasible strategy is to blend polymers with conductive or semiconductive nanomaterials, based on the percolation effect and interfacial polarization effect [7–9]. In recent years, one-dimensional (1D) and two-dimensional (2D) carbon nanomaterials as fillers of polymer dielectric materials have been extensively studied, which are more effective than metal nanoparticles in preparing high dielectric composites [3]. For example, Dang et al. demonstrated a giant dielectric permittivity (>4000 at 1 kHz) at room temperature when the volume fraction of TFP-MWNTs is $f_{\text{TFP-MWNT}} = 0.15$; however, the dielectric constant decreases rapidly (~ 1000 at 10 kHz) as the frequency increases [10]. Huang et al. reported the dielectric properties and breakdown strength of PVDF/graphene ferroelectric composite films, in which the dielectric constant was lower than 150 at 1 kHz and the breakdown strength reduced very quickly with the fillings increasing [9]. Additionally, Shang et al. investigated oriented polyvinylidene fluoride nanocomposites incorporated with graphene nanosheets; a high dielectric constant of 63 is obtained at 100 Hz when the concentration of GNS is 1.27 vol.%, while the electrical breakdown strength of the composite films diminished quickly with a small filling fraction [7]. Using the highly conductive fillers, the relatively high

permittivity always decreased rapidly with increase of the frequency and the breakdown strength declined very quickly at small filler loadings. In recent years, topological insulators, which have a full insulating gap in the bulk and gapless edge or surface states, have drawn more and more attention. Utilizing the characteristics of topological insulators, it is promising to improve the dielectric constant while improving its breakdown field strength.

Topological insulators are new states of quantum matter which cannot be adiabatically connected to conventional insulators and semiconductors. These topological materials have been theoretically predicted and experimentally observed in a variety of systems, including HgTe quantum wells, BiSb alloys, and Bi_2Te_3 and Bi_2Se_3 crystals [11]. Compared with zero- and one-dimensional (0D/1D) nanofillers, 2D nanofillers have a larger aspect ratio, which would improve the dielectric properties of the nanocomposites, since the high surface area and conductivity of 2D nanomaterials in conductor-insulator systems intensively increase polarization densities and interfacial polarization interphases [3, 12, 13]. Chen et al. have demonstrated that 2D Bi_2Te_3 hexagonal nanoplates mixed with PVDF could have high permittivity (about 385 at 1 kHz with 10 vol.% loading of Bi_2Te_3) [8]. Owing to the unique bulk and surface characteristics, it is promising to obtain topological insulator/polymer composite materials with improved permittivity and enhanced breakdown strength. However, there are many kinds of topological insulators found at present, and few of them have been applied in the field of dielectric composite materials.

In this work, 2D Bi_2Se_3 hexagonal nanoplates are chosen as fillers due to their distinctive topological insulation performance and large surface-to-volume ratio. PVDF is used as the polymer matrix since it has a relatively high room temperature dielectric constant and superior ferroelectric properties. The 2D Bi_2Se_3 nanoplates are synthesized through an improved simple "EG-sol" method [14]. Oriented hexagonal Bi_2Se_3 nanoplates with a side length of 400-800 nm are obtained. The nanoplates have a good dispersibility and can be easily dispersed in polar solvents as well as the polymer matrix. To investigate the dielectric properties of Bi_2Se_3/PVDF nanocomposites, composite films with different volume fractions of Bi_2Se_3 nanoplates have been prepared. Due to the percolation effect and interfacial polarization effect, the permittivity of Bi_2Se_3/PVDF nanocomposite films has a sharp increase ($\varepsilon_r = 36$ at 1 kHz) when the loading of 2D Bi_2Se_3 hexagonal nanoplates reaches 13 vol.%. Although the breakdown strength (E_b) declines with the Bi_2Se_3 content, it still maintains a relatively high value (E_b = 255 kV/mm with 2 vol.% Bi_2Se_3) compared to the conductive fillers ($E_b \sim$ 60 kV/mm with 0.3 vol.% graphene and 0.5 vol.% reduced graphene oxide) [7, 9]. The investigation of the Bi_2Se_3/PVDF nanocomposite is conducive to the application of topological insulators in the composite dielectrics.

2. Materials and Methods

2.1. Fabrication of 2D Bi_2Se_3 Nanoplates and Composites. The 2D Bi_2Se_3 nanoplates have been synthesized via an "EG-sol" method, which has been reported earlier [14, 15]. Specifically, 3 mmol bismuth nitrate pentahydrate ($Bi(NO_3)_3{\cdot}5H_2O$), 4.5 mmol sodium selenite (Na_2SeO_3), and 100 ml ethylene glycol (EG) were added to a 250 ml three-neck flask containing a magnetic stirring bar with vigorous stirring followed by refluxing the blended solution at 195°C for 5 h. Then the flask was removed and cooled to room temperature. The product was washed alternately with isopropyl alcohol (IPA) and acetone several times and then dried at 60°C. The preparations of Bi_2Se_3/PVDF nanocomposite films with different Bi_2Se_3 filling fractions are shown in our previous tape-casting methods [16–18].

2.2. Characterization. The TEM image and selected area electron diffraction (SAED) of the Bi_2Se_3 nanoplates are characterized by a TEM (JEM-2100F, JEOL Ltd., Tokyo, Japan) at an accelerating voltage of 200 kV. The cross-sectional and surface microstructure of the composite films are obtained by SEM (MERLIN VP Compact, Zeiss Ltd., Germany) at 15 kV. XRD patterns are performed on a Bruker D8 Advance A25 X-ray diffractometer with Cu Kα radiation (λ = 0.154056 nm) at 40 kV and 200 mA. Before the electrical test, circular gold electrodes with 1 mm radius are prepared on both sides of the films by using ion sputtering equipment (SBC-12, KYKY Technology Co. Ltd., China). The frequency-dependent dielectric constant and loss of the composite films are determined using a precision impedance analyzer (E4980A; Agilent, Palo Alto, CA) at a frequency range of 1 kHz to 2 MHz. Breakdown strength of the nanocomposite films is measured on a ferroelectric test module (TF 2000 analyzer; axiACCT, Germany) at a constant frequency of 100 Hz and gradually increased voltages.

3. Results and Discussion

Figure 1 shows the XRD pattern and standard data card pattern of the Bi_2Se_3 nanoplates. The measured XRD pattern which is presented by the upper black curve is well consistent with the below red line of standard data (PDF#89-2008). The crystal faces corresponding to different diffraction angles have been marked on top of the peaks. No other impurity diffraction peaks are found, which confirms the prepared Bi_2Se_3 nanoparticles have high purity. It is notable that the diffraction peaks corresponding to the crystal faces (0 0 6) and (1 1 6) have higher intensity than the standard card, which indicates the hexagon Bi_2Se_3 nanoplates with a high degree of [0 0 1] preferential orientation [19].

Figures 2(a) and 2(b) show the SEM images of the Bi_2Se_3 nanoplates, which demonstrate that the prepared Bi_2Se_3 nanoplates have excellent dispersibility and a regular hexagon morphology. It is observed that the 2D Bi_2Se_3 hexagonal nanoplates are uniform and have a large aspect ratio. The inserted picture in Figure 2(a) is the Bi_2Se_3 suspension and the corresponding typical Tyndall effect. It reveals that the Bi_2Se_3 nanoplates can be uniformly distributed in DMF solvent, which is beneficial to the fabrication of uniform nanocomposite film.

Figures 3(a) and 3(b) show the representative TEM images of the 2D Bi_2Se_3 nanoplates, which have a hexagonal

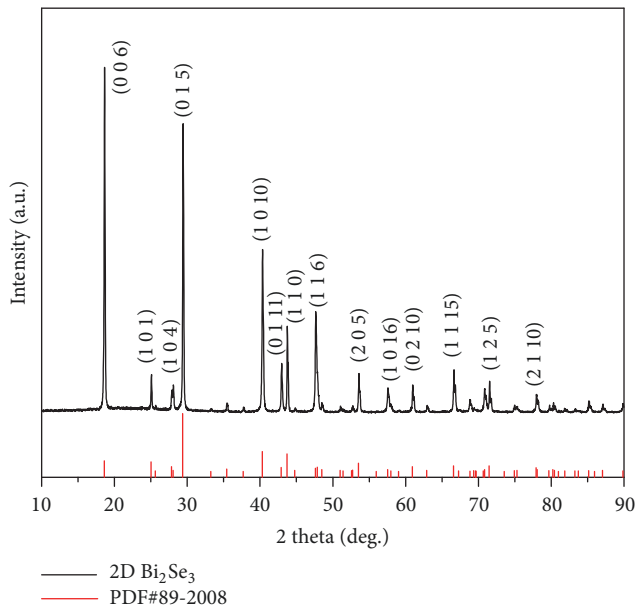

FIGURE 1: XRD pattern and standard data card pattern of Bi_2Se_3 nanoplates.

structure with edge lengths ranging from 400 to 800 nm and thicknesses of 30-70 nm. According to previous studies of Zhang et al., these nanoplates should be several QLs (quintuple layers) [15]. Figure 3(c) is a high-resolution TEM image of a Bi_2Se_3 nanoplate, which shows obvious lattice fringes and illustrates the high crystallinity. The interplanar distance measured from the lattice fringes is 3.58 ± 0.02 Å, as labeled in Figure 3(c), which corresponds well to the (1 0 1) lattice plane of Bi_2Se_3. Figure 3(d) is the SAED pattern of the Bi_2Se_3 nanoplates, which indicates the single crystallinity of the nanoplates.

The dispersion state of fillers in the polymer matrix is an important factor in terms of determining the dielectric behavior of the composite films. Figures 4(a)–4(h) show the cross-sectional SEM images of Bi_2Se_3/PVDF nanocomposite films with increasing Bi_2Se_3 volume fractions from 0 vol.% to 20 vol.%, respectively. Due to the shearing force during the preparation of the SEM sample, the cross-sectional SEM images in Figure 4 show that the nanosheets seem mainly parallel to the cross section, while from the inset in Figure 4(h), which is the surface SEM image of the nanocomposite film with a Bi_2Se_3 loading of 20 vol.%, the bismuth selenide nanosheets are mainly distributed parallel to the surface. It can be seen that the Bi_2Se_3/PVDF composite films with 0-20 vol.% Bi_2Se_3 fillings are dense and uniform except a few holes in the composite film with 20 vol.% Bi_2Se_3. Besides, 2D Bi_2Se_3 hexagonal nanoplates are uniformly and randomly dispersed in the PVDF polymer, which exhibit excellent compatibility with the polymer matrix. Due to the high aspect ratio of the 2D Bi_2Se_3 hexagonal nanoplates, the dense combination between the fillers and polymer matrix can generate a large number of interfaces, which is beneficial to improve the dielectric constant. Additionally, when the Bi_2Se_3 volume fraction reaches 15 vol.% and 20 vol.%, the space among the nanoplates becomes small and the insulated PVDF polymer is thinner, as shown in Figures 4(g) and 4(h).

Figure 5 shows the XRD pattern of several typical films. The XRD curve of pure PVDF illustrates that PVDF film has a dominant β phase and a little α phase. Additionally, XRD patterns of the Bi_2Se_3/PVDF composite films indicate stable rhombohedral Bi_2Se_3. As the content of the filler particle increases, the diffraction peaks of the composite films become more intense. Comparing to the XRD pattern of Bi_2Se_3 nanoplates, the diffraction peaks corresponding to the crystal faces (0 0 6) and (1 1 6) have higher intensity. This could be attributed to the casting effect of solution and confinement effect of Bi_2Se_3 into the polymer network [20]. In other words, Bi_2Se_3 nanoplates with [0 0 1] orientation tend to be distributed parallel to the surface of the composite film, which is well consistent with the surface SEM result of the composite film.

Figure 6(a) shows the frequency dependence of the dielectric constant for the Bi_2Se_3/PVDF nanocomposite films with different composition. The dielectric constant is relatively stable over the total measured frequency range (1 kHz-2 MHz) and increases with the BS (Bi_2Se_3) content, which is almost independent of frequency, comparing with GNS/PVDF (graphene nanosheets/polyvinylidene fluoride) nanocomposites [7], PVDF/rGO (polyvinylidene fluoride/reduced graphene oxide) composite films [9], and TFP-MWNTs/PVDF (trifluorophenyl-multiwalled carbon nanotubes/polyvinylidene fluoride) nanocomposites [10]. It is worth noting that the permittivity of the composite films maintains 8-16 with 0-12 vol.% Bi_2Se_3 content and increases sharply (ε_r ~36 at 1 kHz) when the 2D Bi_2Se_3 nanoplates reach a volume fraction of 13 vol.%. The dielectric constant is 950 at 1 kHz when the volume fraction of the 2D Bi_2Se_3 nanoplates is 20 vol.%, which is two orders of magnitude higher than the pure PVDF polymer matrix (ε_r ~8.5 at 1 kHz). It is mainly attributed to the interfacial polarization effects and the percolation effects of the fillers. When the volume fraction of the Bi_2Se_3 nanoplates is below 12 vol.%, the slow increase of permittivity with Bi_2Se_3 loading can be ascribed to the interfacial polarization because the Bi_2Se_3 nanoplates have a conductive surface and a large aspect ratio. The dramatic increase in the permittivity should be attributed to the percolation effects. When the Bi_2Se_3 content reaches 13 vol.%, the conductive surface of the Bi_2Se_3 nanoplates is connected and therefore forms a framework which enables the high speed transmission of the electrons. Figure 6(b) shows that the dielectric loss is low and relatively stable when the Bi_2Se_3 content is below 12 vol.%. Then it drastically increases when the Bi_2Se_3 content reaches 13 vol.%, which corresponds well with the change for the dielectric constant. Figure 6(c) shows the change of dielectric constant and dielectric loss with the variation of Bi_2Se_3 content. It clearly shows the abrupt increase of the dielectric constant and loss at 13 vol.%, which represents the percolation threshold of the Bi_2Se_3/PVDF system and coincides with the literature value for Bi_2Te_3 [8]. However, according to previous literature reports, the percolation threshold of this work (13 vol.%) is larger than most of the carbon nanotubes and graphene

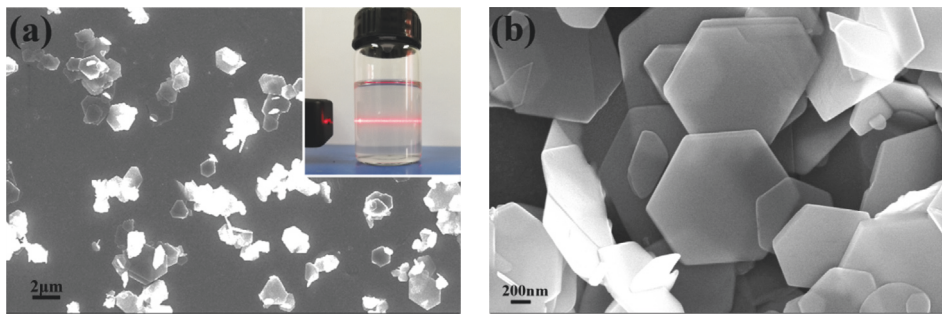

(a) (b)

Figure 2: ((a), (b)) SEM images of the Bi_2Se_3 nanoplates; the inserted picture in Figure 2(a) is the Bi_2Se_3 suspension and the corresponding Tyndall effect.

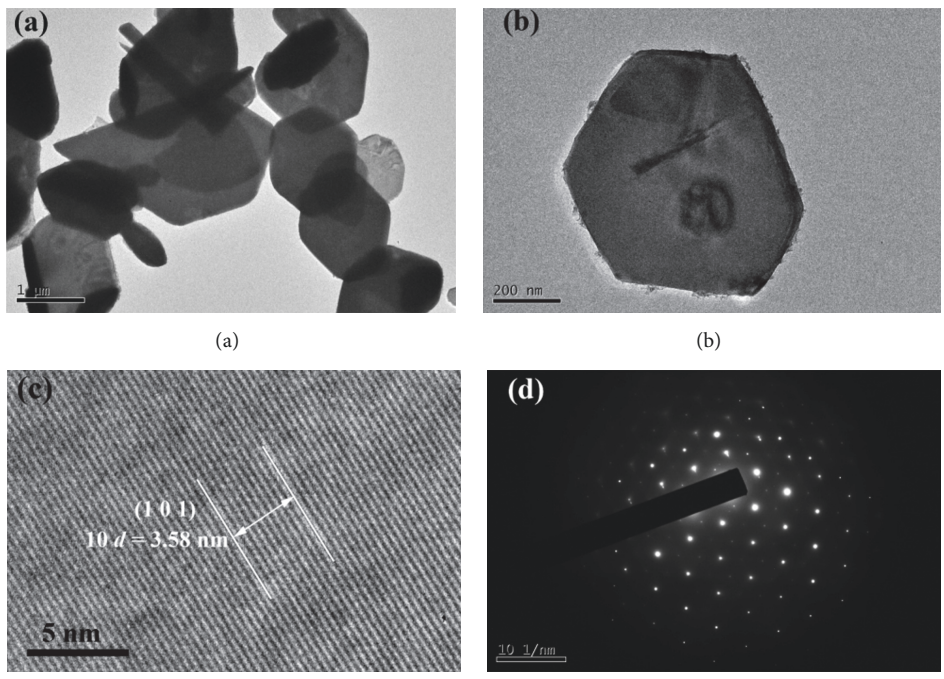

(a) (b)

(c) (d)

Figure 3: ((a), (b)) TEM images, (c) high-resolution TEM image, and (d) SAED pattern of Bi_2Se_3 nanoplates.

loaded PVDF-based nanocomposites (generally <10 vol.%). For example, the percolation threshold of GNS/PVDF and TFP-MWNT/PVDF nanocomposites are 1.27 vol.% and 8 vol.%, respectively [7, 10]. In this case, the higher percolation threshold may be a consequence of three factors. (i) Due to the casting effect of solution, Bi_2Se_3 nanoplates tend to form preferred alignment and be distributed parallel to the surface of the composite film, which has been verified by SEM and XRD results. Therefore, the probability of contact between Bi_2Se_3 nanoplates is reduced, which makes it more difficult to form a conductive network [1]. (ii) The highly insulating Bi_2Se_3 nanoplates in the bulk obstruct the transmission of the electrons and thus more Bi_2Se_3 nanoplates are needed to provide a comparable conductive surface region. (iii) Compared with most of the carbon nanotubes and graphene fillers, aspect ratios of the prepared Bi_2Se_3 nanoplates are lower, and a smaller aspect ratio generally corresponds to a higher percolation threshold [21].

Dependence of the conductivity of the Bi_2Se_3/PVDF nanocomposite films on the BS (Bi_2Se_3) volume fraction is measured and shown in Figure 7. The conductivity values are relatively low with Bi_2Se_3 loading lower than 12 vol.%, which illustrates that the composite films are highly insulated. The slow increase of permittivity with Bi_2Se_3 loading can be ascribed to the interfacial polarization and the large aspect ratio of the Bi_2Se_3 nanoplates. When the Bi_2Se_3 content is equal to or greater than 13 vol.%, the conductivity sharply increases. At this point, an insulator-conductor transition occurs. As topological insulator Bi_2Se_3 nanoplates are characterized by a full insulating gap in the bulk and gapless edge or surface states, the conductive edge or surface of the Bi_2Se_3 nanoplates could be considered as numerous

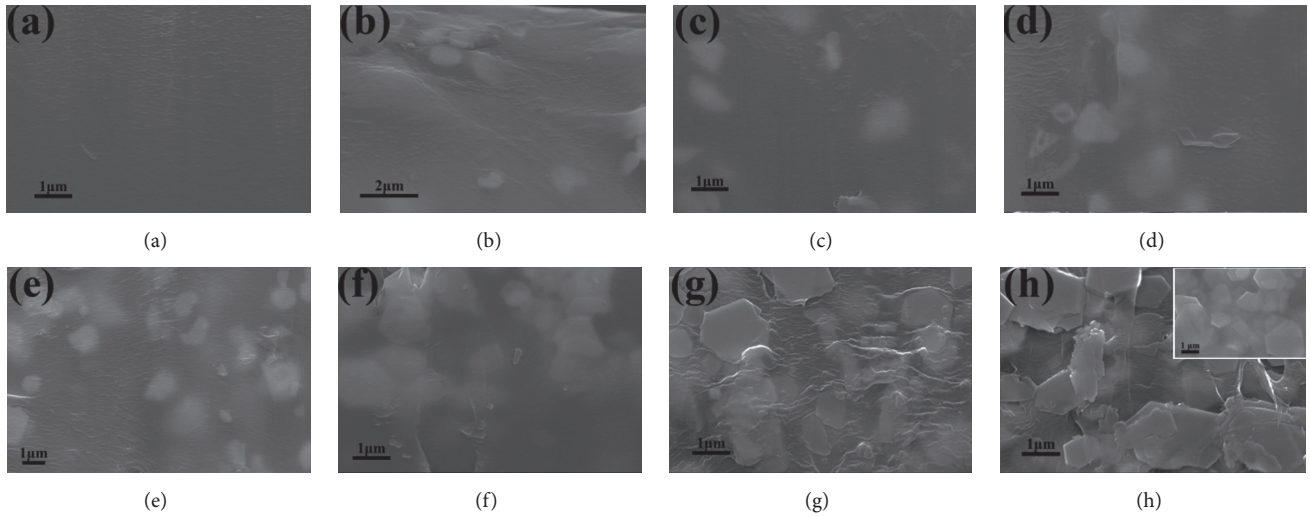

FIGURE 4: Cross-sectional SEM images of the Bi_2Se_3/PVDF nanocomposite films with Bi_2Se_3 volume fractions of (a) 0 vol.%, (b) 2 vol.%, (c) 4 vol.%, (d) 6 vol.%, (e) 8 vol.%, (f) 10 vol.%, (g) 15 vol.%, and (h) 20 vol.%.

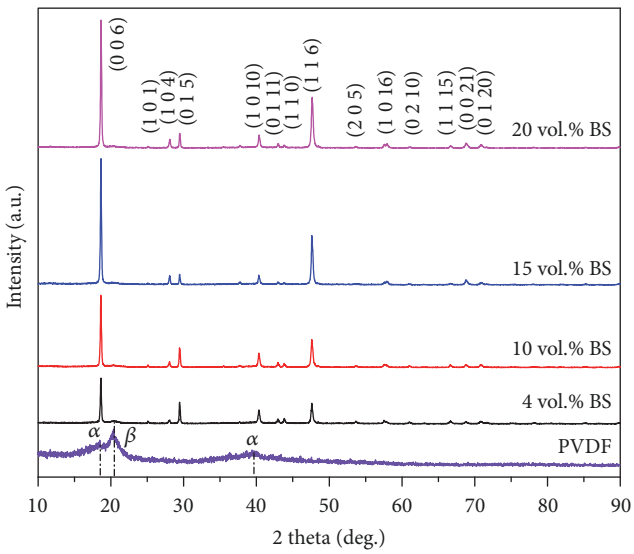

FIGURE 5: XRD pattern of pure PVDF film and the representative Bi_2Se_3/PVDF composite films filled with 4 vol.%, 10 vol.%, 15 vol.%, and 20 vol.% Bi_2Se_3 nanoplates.

electrodes within a thin insulating PVDF polymer, together comprising a micro-capacitor model [22, 23]. These micro-capacitors greatly improve the macro dielectric constant. Therefore, the prepared Bi_2Se_3/PVDF composite films could act as an ideal candidate of high permittivity materials in high charge storage capacitors [24]. When the Bi_2Se_3 content is over the percolation threshold, in this work 13 vol.%, the dielectric constant continues to rise from 36 to 950 and the dielectric loss also increases from 11 to 14000 at 1 kHz. The conductivity networks have a great effect on the dielectric loss. The composite films with low Bi_2Se_3 content are still insulating materials and show low dielectric loss similarly to the PVDF matrix. With the increasing Bi_2Se_3 nanoplates, the relative content of the polymer is too small to constitute an insulation system; edge or surface conductive topological insulator Bi_2Se_3 hexagonal nanoplates begin to touch each other and form conductive networks where the leakage current abruptly increases; as a result the dielectric loss increases dramatically. In addition, when the Bi_2Se_3 content of the composites is from 13 vol.% to 20 vol.%, the dielectric loss decreases with the increase of frequency because the induced space charges can difficultly follow the reversing field, leading to the reduced electronic oscillations [7]. These high-dielectric-constant and high-dielectric-loss composite films could be applied in an electromagnetic-wave absorption field [25–27].

For dielectric applications, the breakdown strength is an important parameter to evaluate the novel composite dielectric materials. Figure 8 illustrates the histogram of breakdown strength as a function of Bi_2Se_3 volume fraction. As the composite films with Bi_2Se_3 loading of 13 vol.% to 20 vol.% have too small resistance to measure their applied voltage, only the breakdown field of the films with volume fraction of 0-12 vol.% is measured. As can be seen from the histogram, the breakdown strength of pure PVDF is 315 kV/mm. The breakdown strength decreases with the increase of the Bi_2Se_3 content, which can be ascribed to the space charges introduced by the conductive edge or surface of Bi_2Se_3 nanoplates. Based on the report of Gyure and Beale [28], the reduction in breakdown strength is attributed to the agglomeration of conductive particles and short-circuiting of some regions in the nanocomposites, which causes the voltage drop sharply in regions and leads to a locally enhanced electric field. Therefore the breakdown will occur at a relatively low macroscopic electric field [29]. For this work, when the loaded Bi_2Se_3 volume fraction is low (no more than 2 vol.%), Bi_2Se_3 nanoplates are well separated by polymer and the interparticle distance is relatively large. However, as the concentration increases (greater than or equal to 4 vol.%), the Bi_2Se_3 nanoplates are close enough to

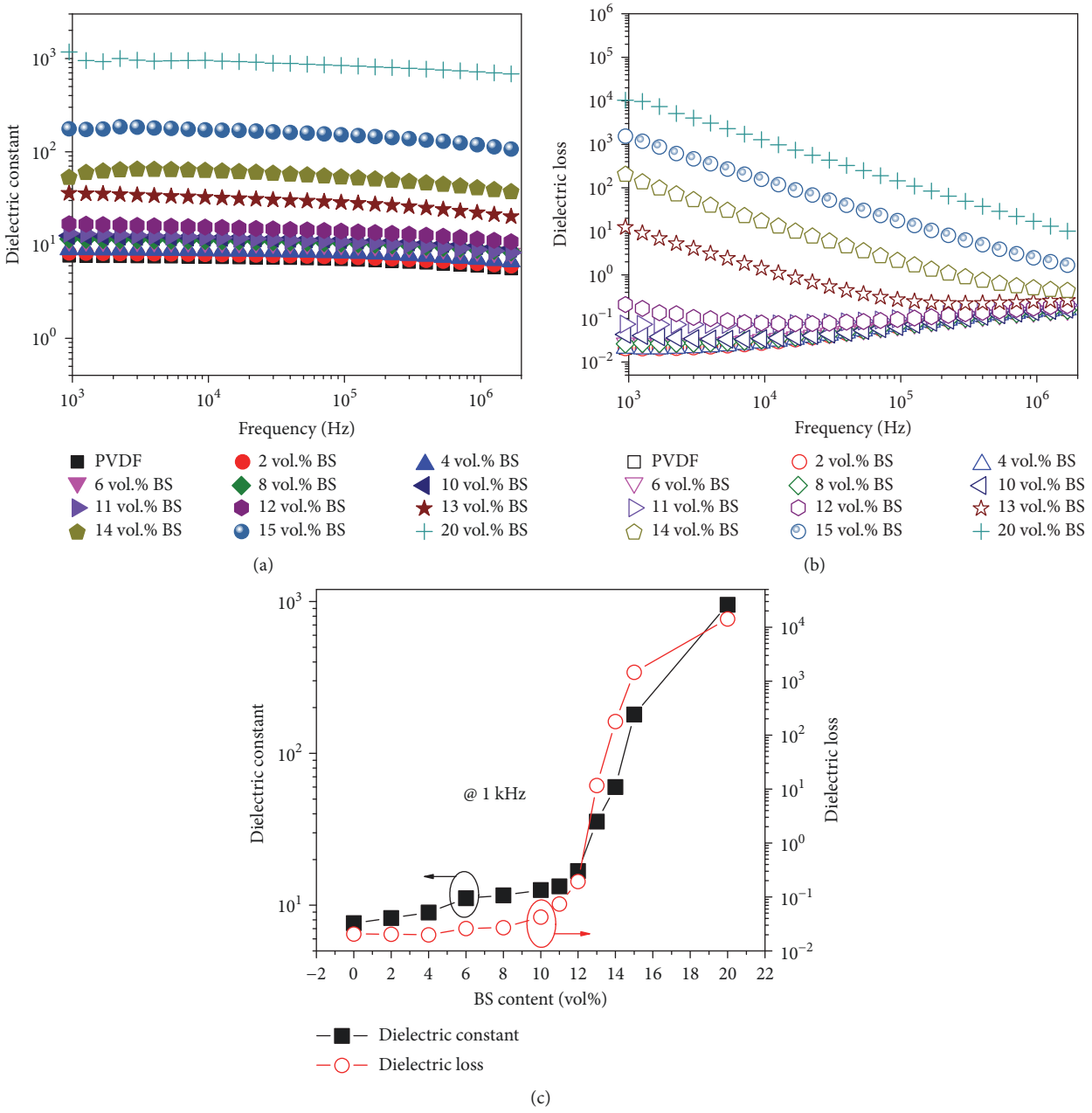

FIGURE 6: Frequency dependence of (a) dielectric constant and (b) dielectric loss of the Bi_2Se_3/PVDF nanocomposite films with different composition. (c) BS (Bi_2Se_3) content dependence of dielectric constant and dielectric loss of the Bi_2Se_3/PVDF nanocomposite films, measured at room temperature and 1 kHz.

aggregate and form large clusters to generate a short-circuit area in the composite, inducing a sharp drop in breakdown strength. It is worth noting that the breakdown strength only slightly decreases when the volume fraction of Bi_2Se_3 increases from 0 to 2 vol.%, which is different from other carbon filling composite materials, owing to the unique full insulating gap in the bulk of Bi_2Se_3 topological insulators. Owing to the macroscopically insulating behavior of the composite films with Bi_2Se_3 content up to 12 vol.%, these conductor-insulator composites can be used in capacitive and energy storage applications [30–32].

4. Conclusions

In summary, topological insulator 2D Bi_2Se_3 nanoplates with a full insulating gap in the bulk and gapless edge or surface states and PVDF blend films have been prepared. The dielectric performance of Bi_2Se_3/PVDF nanocomposite films is studied. Due to the large aspect ratio of the 2D Bi_2Se_3 nanoplates and the percolation effect, both the dielectric constant and loss of the Bi_2Se_3/PVDF nanocomposite films maintain a relatively low value with the Bi_2Se_3 content lower than 12 vol.% and drastically increase with the Bi_2Se_3 content

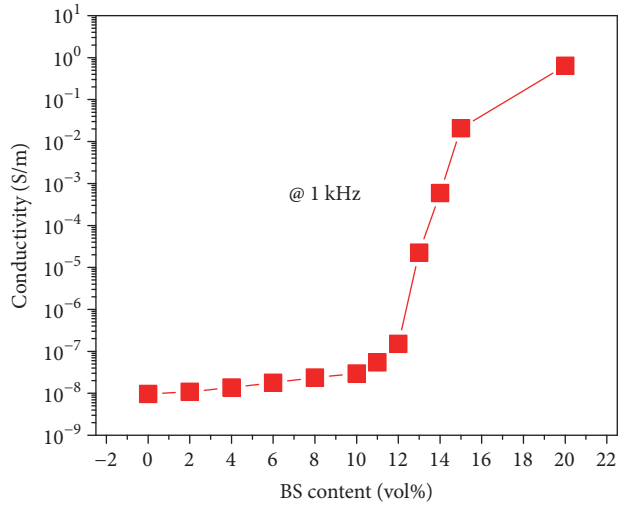

FIGURE 7: Conductivity variation of the Bi_2Se_3/PVDF nanocomposite films with respect to the BS (Bi_2Se_3) volume fraction, measured at room temperature and 1 kHz.

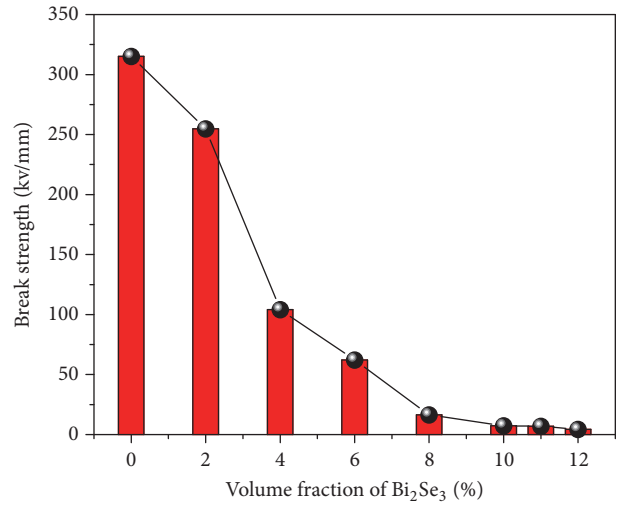

FIGURE 8: Histogram of breakdown strength as a function of Bi_2Se_3 volume fraction.

higher than 13 vol.%. A giant dielectric constant of 950 is obtained at 1 kHz with 20 vol.% Bi_2Se_3 loading, which is 110 times that of the pure PVDF film. In addition, the breakdown strength of the composites has been investigated and the sharp drop in the electrical breakdown strength depending upon the concentration of the Bi_2Se_3 nanoplates is attributed to agglomeration effects. The Bi_2Se_3/PVDF nanocomposite films constitute a novel type of topological insulator-based composite materials and are conducive to the investigation of high-performance dielectrics.

Data Availability

The data used to support the findings of this study are included within the article.

Conflicts of Interest

The authors declare that there are no conflicts of interest regarding the publication of this paper.

Acknowledgments

This work was supported by the National Natural Science Foundation of China (Grant Nos. 51802023, 61774020, and 51802021), Young Elite Scientists Sponsorship Program by CAST (Grant No. 2018QNRC001), Science and Technology Plan of Shenzhen City (Grant No. 201887776), Fund of IPOC BUPT (Grant No. IPOC2017ZT06), and State Key Laboratory of New Ceramic and Fine Processing, Tsinghua University (No. KF201803).

References

[1] J.-K. Yuan, S.-H. Yao, Z.-M. Dang, A. Sylvestre, M. Genestoux, and J. Bai, "Giant dielectric permittivity nanocomposites: Realizing true potential of pristine carbon nanotubes in polyvinylidene fluoride matrix through an enhanced interfacial interaction," *The Journal of Physical Chemistry C*, vol. 115, no. 13, pp. 5515–5521, 2011.

[2] K. Bi, D. Yang, J. Chen et al., "Experimental demonstration of ultra-large-scale terahertz all-dielectric metamaterials," *Photonics Research*, vol. 7, no. 4, p. 457, 2019.

[3] Z.-M. Dang, M.-S. Zheng, and J.-W. Zha, "1D/2D carbon nanomaterial-polymer dielectric composites with high permittivity for power energy storage applications," *Small*, vol. 12, no. 13, pp. 1688–1701, 2016.

[4] X. Zhang, Y. Huan, K. Li et al., "Enhanced photocatalytic activity and cycle stability driven by ultrasonic vibration for ferroelectric photocatalysts," *IET Nanodielectrics*, vol. 2, no. 1, pp. 48–53, 2019.

[5] C. Wu, X. Huang, X. Wu, L. Xie, K. Yang, and P. Jiang, "Graphene oxide-encapsulated carbon nanotube hybrids for high dielectric performance nanocomposites with enhanced energy storage density," *Nanoscale*, vol. 5, no. 9, pp. 3847–3855, 2013.

[6] S. Luo, Y. Shen, S. Yu et al., "Construction of a 3D-BaTiO 3 network leading to significantly enhanced dielectric permittivity and energy storage density of polymer composites," *Energy & Environmental Science*, vol. 10, no. 1, pp. 137–144, 2017.

[7] J. Shang, Y. Zhang, L. Yu, B. Shen, F. Lv, and P. K. Chu, "Fabrication and dielectric properties of oriented polyvinylidene fluoride nanocomposites incorporated with graphene nanosheets," *Materials Chemistry and Physics*, vol. 134, no. 2-3, pp. 867–874, 2012.

[8] J. Chen, X. Wang, X. Yu et al., "High dielectric constant and low dielectric loss poly (vinylidene fluoride) nanocomposites via a small loading of two-dimensional Bi 2 Te 3@ Al 2 O 3 hexagonal nanoplates," *Journal of Materials Chemistry C*, vol. 6, no. 2, pp. 271–279, 2018.

[9] L. Huang, C. Lu, F. Wang, and L. Wang, "Preparation of PVDF/graphene ferroelectric composite films by in situ reduction with hydrobromic acids and their properties," *RSC Advances*, vol. 4, no. 85, pp. 45220–45229, 2014.

[10] Z. Dang, L. Wang, Y. Yin, Q. Zhang, and Q. Lei, "Giant dielectric permittivities in functionalized carbon-nanotube/

electroactive-polymer nanocomposites," *Advanced Materials*, vol. 19, no. 6, pp. 852–857, 2007.

[11] X.-L. Qi and S.-C. Zhang, "Topological insulators and superconductors," *Reviews of Modern Physics*, vol. 83, no. 4, pp. 1057–1110, 2011.

[12] C. Jiang, D. Zhang, K. Zhou, X. Zhou, H. Luo, and I. Abrahams, "Significantly enhanced energy storage density of sandwich-structured (Na0.5Bi0.5)0.93Ba0.07TiO3/P(VDF–HFP) composites induced by PVP-modified two-dimensional platelets," *Journal of Materials Chemistry A*, vol. 4, no. 46, pp. 18050–18059, 2016.

[13] D. Zhang, W. Liu, L. Tang, K. Zhou, and H. Luo, "High performance capacitors via aligned TiO2 nanowire array," *Applied Physics Letters*, vol. 110, no. 13, Article ID 133902, 2017.

[14] C. Dun, C. A. Hewitt, H. Huang et al., "Layered Bi2Se3 nanoplate/polyvinylidene fluoride composite based n-type thermoelectric fabrics," *ACS Applied Materials & Interfaces*, vol. 7, no. 13, pp. 7054–7059, 2015.

[15] J. Zhang, Z. Peng, A. Soni et al., "Raman spectroscopy of few-quintuple layer topological insulator Bi2Se3 nanoplatelets," *Nano Letters*, vol. 11, no. 6, pp. 2407–2414, 2011.

[16] Z. Feng, Y. Hao, M. Bi, Q. Dai, and K. Bi, "Highly dispersive Ba 0.6 Sr 0.4 TiO 3 nanoparticles modified P (VDF-HFP)/PMMA composite films with improved energy storage density and efficiency," *IET Nanodielectrics*, vol. 1, no. 1, pp. 60–66, 2018.

[17] M. Bi, Y. Hao, J. Zhang, M. Lei, and K. Bi, " Particle size effect of BaTiO 3 nanofillers on the energy storage performance of polymer nanocomposites ," *Nanoscale*, vol. 9, no. 42, pp. 16386–16395, 2017.

[18] K. Bi, M. Bi, Y. Hao et al., "Ultrafine core-shell BaTiO3@SiO2 structures for nanocomposite capacitors with high energy density," *Nano Energy*, vol. 51, pp. 513–523, 2018.

[19] Y. Sun, H. Cheng, S. Gao et al., "Atomically thick bismuth selenide freestanding single layers achieving enhanced thermoelectric energy harvesting," *Journal of the American Chemical Society*, vol. 134, no. 50, pp. 20294–20297, 2012.

[20] F. Macedonio, A. Politano, E. Drioli, and A. Gugliuzza, "Bi2Se3-assisted membrane crystallization," *Materials Horizons*, vol. 5, no. 5, pp. 912–919, 2018.

[21] S. Yao, Z. Dang, M. Jiang, H. Xu, and J. Bai, "Influence of aspect ratio of carbon nanotube on percolation threshold in ferroelectric polymer nanocomposite," *Applied Physics Letters*, vol. 91, no. 21, p. 212901, 2007.

[22] F. He, S. Lau, H. L. Chan, and J. Fan, "High dielectric permittivity and low percolation threshold in nanocomposites based on poly(vinylidene fluoride) and exfoliated graphite nanoplates," *Advanced Materials*, vol. 21, no. 6, pp. 710–715, 2009.

[23] J. Yuan, Z. Dang, S. Yao et al., "Fabrication and dielectric properties of advanced high permittivity polyaniline/poly(vinylidene fluoride) nanohybrid films with high energy storage density," *Journal of Materials Chemistry*, vol. 20, no. 12, p. 2441, 2010.

[24] C. R. Mulzer, L. Shen, R. P. Bisbey et al., "Superior charge storage and power density of a conducting polymer-modified covalent organic framework," *ACS Central Science*, vol. 2, no. 9, pp. 667–673, 2016.

[25] D. D. L. Chung, "Carbon materials for structural self-sensing, electromagnetic shielding and thermal interfacing," *Carbon*, vol. 50, no. 9, pp. 3342–3353, 2012.

[26] K. Bi, X. Wang, Y. Hao, M. Lei, G. Dong, and J. Zhou, "Wideband slot-coupled dielectric resonator-based filter," *Journal of Alloys and Compounds*, vol. 785, pp. 1264–1269, 2019.

[27] H. Xu, K. Bi, Y. Hao et al., "Switchable complementary diamond-ring-shaped metasurface for radome application," *IEEE Antennas and Wireless Propagation Letters*, vol. 17, no. 12, pp. 2494–2497, 2018.

[28] M. F. Gyure and P. D. Beale, "Dielectric breakdown in continuous models of metal-loaded dielectrics," *Physical Review B: Condensed Matter and Materials Physics*, vol. 46, no. 7, pp. 3736–3746, 1992.

[29] H. Stoyanov, D. Mc Carthy, M. Kollosche, and G. Kofod, "Dielectric properties and electric breakdown strength of a subpercolative composite of carbon black in thermoplastic copolymer," *Applied Physics Letters*, vol. 94, no. 23, Article ID 232905, 2009.

[30] X. Wang, Y. Cui, T. Li, M. Lei, J. Li, and Z. Wei, "Recent advances in the functional 2D photonic and optoelectronic devices," *Advanced Optical Materials*, vol. 7, no. 3, Article ID 1801274, 2018.

[31] Z.-S. Wu, G. Zhou, L.-C. Yin, W. Ren, F. Li, and H.-M. Cheng, "Graphene/metal oxide composite electrode materials for energy storage," *Nano Energy*, vol. 1, no. 1, pp. 107–131, 2012.

[32] S. Lin, H. Wang, X. Zhang et al., "Direct spray-coating of highly robust and transparent Ag nanowires for energy saving windows," *Nano Energy*, vol. 62, pp. 111–116, 2019.